Science and Technology Infusion Climate Bulletin
NOAA's National Weather Service
36th NOAA Annual Climate Diagnostics and Prediction Workshop
Fort Worth, TX, 3-6 October 2011

Precipitation Characteristics of the South American Monsoon System Derived from Multiple Data Sets

Leila M. V. Carvalho[1, 2], Charles Jones[2], Adolfo N. D. Posadas[3],
Roberto Quiroz[3], Bodo Bookhagen[1, 2] and Brant Liebmann[4]

[1]*Department of Geography, University of California, Santa Barbara, CA, USA*
[2]*Earth Research Institute, University of California, Santa Barbara, CA, USA*
[3]*International Potato Center (CIP), Lima, Peru*
[4]*CIRES Climate Diagnostics Center, Boulder, CO, USA*

1. Introduction

The monsoon (hereafter, South American Monsoon System, SAMS) is the most important climatic feature in South America (Zhou and Lau 1998; Vera *et al.* 2006; Marengo *et al.* 2010). The main feature of the SAMS is the enhanced convective activity and heavy precipitation in tropical South America, which typically starts in October-November, is fully developed during December-February and retreats in late April or early May (Kousky 1988; Horel *et al.* 1989; Marengo *et al.* 2001; Grimm *et al.* 2005; Gan *et al.* 2006; Liebmann *et al.* 2007).

Although the variability of precipitation in the SAMS has been extensively investigated over the years, one of the main challenges has been the availability of data sets with suitable spatial and temporal resolutions able to resolve the large range of meteorological systems observed during the monsoon. While some stations in South America have precipitation records going back several decades, the sparseness of stations is not adequate to characterize mesoscale precipitation systems. To overcome this difficulty, some studies have developed considerable efforts to collect precipitation records from stations and develop quality-controlled gridded precipitation data sets (Legates and Willmott 1990; Liebmann and Allured 2005; Silva *et al.* 2007).

Recently, new generation of reanalysis products have been completed (Saha *et al.* 2010; Dee *et al.* 2011; Rienecker *et al.* 2011). The new reanalyses, which are derived from state-of-the-art data assimilation systems and high resolution climate models, provide substantial improvements in the spatiotemporal variability of precipitation relative to the first generation of reanalyses (Higgins *et al.* 2010; Saha *et al.* 2010; Rienecker *et al.* 2011; Silva *et al.* 2011).

This paper evaluates and compares statistical properties of daily precipitation in three types of data sets: gridded station data, satellite-derived precipitation and reanalyses. This study employs several analyses to determine consistencies and disagreements in the representation of precipitation over SAMS. The period 1998-2008 is selected in order to minimize missing data and develop a consistent comparison among the data sets. In addition, since the data sets are available with different horizontal resolutions, the comparison is performed in two ways: 1) all data sets regridded to a common resolution and 2) data sets with their original resolutions.

2. Data

The statistical properties of precipitation in the SAMS region are investigated with daily gridded data from multiple sources during 1 Jan-31 Dec 1998-2008. The following data sets are used:

i) Physical Sciences Division, Earth System Research Laboratory (PSD): This data set is formed from observed precipitation collected at stations distributed over South America (Liebmann and Allured 2005, 2006). The daily gridded precipitation is constructed by averaging all observations available within a specified radius of each grid point. Two grid resolutions (1° and 2.5° lat/lon) are used in this study.

Correspondence to: Leila M. V. Carvalho, Department of Geography, University of California, Santa Barbara, CA 93106, USA; Email: leila@eri.ucsb.edu.

ii) Global Precipitation Climatology Project (GPCP): The daily GPCP combines Special Sensor/Microwave Imager (SSM/I), GPCP Version 2.1 Satellite-Gauge, geosynchronous-orbit Infrared (IR), (geo-IR) Tb histograms (1°x1° grid in the band 40°N-40°S, 3-hourly), low-orbit IR GOES Precipitation Index (GPI), TIROS Operational Vertical Sounder (TOVS) and Atmospheric Infrared Sounder (AIRS) data (Huffman *et al.* 2001). The GPCP data used in this study have 1^{o} lat/lon grid spacing.

iii) Climate Prediction Center unified gauge (CPC-uni): The NOAA Climate Prediction Center (CPC) unified gauge uses an optimal interpolation technique to re-project precipitation reports to a grid (Higgins *et al.* 2000; Silva *et al.* 2007; Chen *et al.* 2008; Silva *et al.* 2011). This study uses data with 0.5^{o} lat/lon grid spacing. Although the PSD and CPC-uni data sets share some of the same station observations, it is worth noting that the quality control and gridding methods are distinct. In addition, it is likely that the number and origin of station data in both data sets are different.

iv) Climate Forecast System Reanalysis (CFSR): Daily precipitation from the NCEP CFSR (Saha *et al.* 2010) is used at 0.5^{o} lat/lon grid spacing. It is also important to note that precipitation is not assimilated in the CFSR production and is a forecast (first-guess) product.

v) Modern-Era Retrospective Analysis for Research and Applications (MERRA): Daily precipitation from MERRA at 0.5^{o} latitude/0.3^{o} longitude is used (Rienecker *et al.* 2011). As in the CFSR, precipitation is a forecast product.

vi) Tropical Rainfall Measurement Mission (TRMM 3B42 V6): Daily precipitation from TRMM is used with 0.25^{o} lat/lon (Bookhagen and Strecker 2008; Bookhagen and Strecker 2010; Bookhagen and Burbank 2011).

3. Results

Several statistical analysis have been applied to the daily precipitation and the reader is referred to Carvalho *et al.* (2011) for additional details. The annual evolution of SAMS is examined to determine consistencies and disagreements among the data sets. The large-scale features of interest are: the dominant spatial precipitation pattern, dates of onset and demise, duration and amplitude of the monsoon. These characteristics are determined with empirical orthogonal functional (EOF) analysis applied to the daily precipitation (only land grid points) from each data set separately. Before computation of EOF analysis, the time series of precipitation in each grid point are scaled by the square-root of the cosine of the latitude and the long-term mean removed (1 Jan-31 Dec, 1998-2008). The first mode (EOF1) and associated temporal coefficient (PC1) explain the largest fraction of the total variance of precipitation over land and are used to describe the annual evolution of SAMS.

To determine dates of onset, demise and duration of SAMS, the daily PC1 is smoothed with ten passes of a 15-day moving average. This smoothing procedure is obtained empirically and used to decrease the influence of high frequency variations during the transition phases of SAMS. The large-scale onset of SAMS is defined as the date when the smoothed PC1 changes from negative to positive values. This implies that positive precipitation anomalies during that time become dominant over the SAMS domain. Likewise, the demise of SAMS is defined as the date when the smoothed PC1 changes from positive to negative values. The duration of the monsoon is defined as the period between onset and demise dates. The seasonal amplitude of the monsoon is defined as the integral of positive unsmoothed PC1 values from onset to demise. Therefore, the seasonal amplitude index represents the sum of positive precipitation anomalies and minimizes the effect of "break" periods in the monsoon especially near the onset and demise. Active/break periods in SAMS are particularly frequent on intraseasonal time scales (Jones and Carvalho 2002).

Figure 1 shows the spatial patterns of EOF1 derived from each data set with 2.5^{o} lat/lon grid spacing and expressed as correlations between PC1 and precipitation anomalies. Positive correlations are interpreted as positive precipitation anomalies and indicative of active SAMS. In general, all data sets show similar features such as positive precipitation anomalies over central South America and negative anomalies over the northern parts of the continent. The region of negative anomalies over northern South America is substantially smaller in the PSD due to missing data (the "bull's eye" at ~60^{o}W, 10^{o}S is a grid point with missing data). The magnitude of positive correlations varies slightly and is highest for PSD. The largest positive correlation in MERRA is slightest to the west relative to the other data sets.

The percentages of explained variance by EOF1 are: 20.5% (PSD), 11.6% (GPCP), 8.4% (CPC-uni), 10% (CFSR), 17.9% (MERRA) and 6.9% (TRMM). EOF1 captures the largest fraction of the total variance, which includes subseasonal, seasonal and interannual variations, since the EOF analysis is performed removing only the long-term mean. Main differences in explained variance are associated with how much each PC1 represents the distribution of subseasonal, seasonal and interannual variations. These percentages are comparable to the percentages obtained with the data sets at their original resolutions, which suggests that spatial resolution of the data sets is not the main issue, but rather how each data set represents temporal variations.

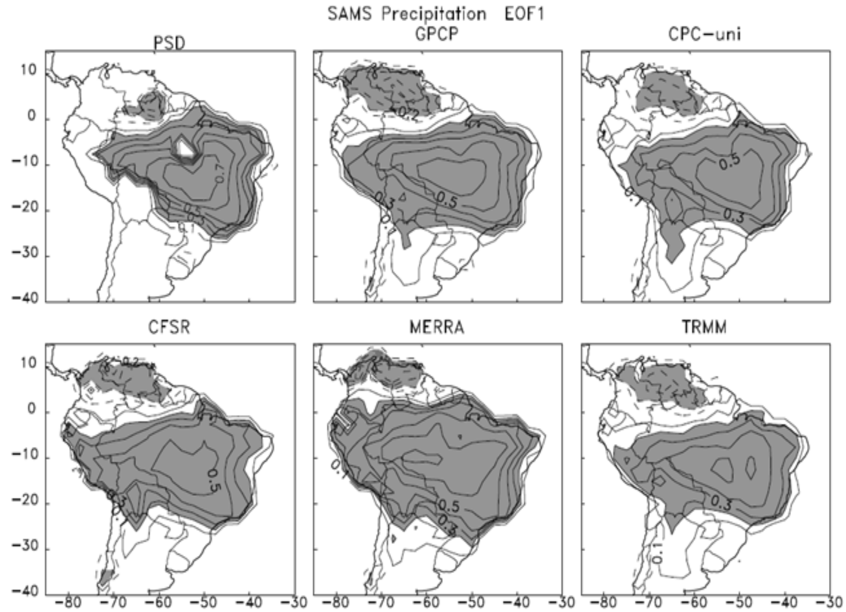

Fig. 1 First EOF patterns described as correlations between the first temporal coefficient (PC1) and precipitation anomalies. Solid (dashed) contours indicate positive (negative) correlations at 0.1 intervals (zero contours omitted). Shadings indicate correlations ≥ 0.2 (≤ -0.2) and are significant at 5%. Data grid spacing: 2.5° lat/lon.

Dates of onset, demise and duration of SAMS derived from each data set with the original resolution are shown in Fig. 2. The mean onset date (Fig.2 top) is highly coherent among PSD, GPCP, CPC-uni and TRMM (~21 October) including the ranges of minimum and maximum onset dates. In contrast, the mean onset dates in CFSR and MERRA are off by several weeks. The variability in dates of mean demise (Fig. 2 middle) indicates agreements among PSD, GPCP, CPC-uni and TRMM and some differences in CFSR and large disagreement in MERRA. Consequently, the mean durations of SAMS (~180 days) agree reasonably well among PSD, GPCP, CPC-uni and TRMM data and is shorter and more variable in the CFSR and MERRA reanalyses (Fig. 2 bottom). These results indicate that differences in data resolution do not explain disagreements in the annual evolution of SAMS especially between CFSR and MERRA and the other data sets.

5. Conclusions

Carvalho *et al.* (2011) compares some statistical properties of daily gridded precipitation from different data (1998-2008): 1) Physical Sciences Division, Earth System Research Laboratory (PSD) (1.0^o and 2.5^o lat/lon), 2) Global Precipitation Climatology Project (GPCP at 1^o lat/lon), 3) Climate Prediction Center unified gauge (CPC-uni) (0.5^o lat/lon), 4) NCEP CFSR reanalysis (0.5^o lat/lon), 5) NASA MERRA reanalysis (0.5^o lat/0.3^o lon) and 6) TRMM 3B42 V6 data (0.25^o lat/lon). The same statistical analyses are applied to data in: 1) a common 2.5^o lat/lon grid and 2) in the original resolutions of the data sets.

All data sets consistently represent the large-scale patterns of the SAMS. The onset, demise and duration of SAMS are consistent among PSD, GPCP, CPC-uni and TRMM data sets, whereas CFSR and MERRA seem to have problems in capturing the correct timing of SAMS. Power spectrum analysis shows that intraseasonal variance is somewhat similar in the six data sets. Moreover, differences in spatial patterns of mean precipitation are small among PSD, GPCP, CPC-uni and TRMM data and some discrepancies are found CFSR and MERRA. Fitting of gamma frequency distributions to daily precipitation shows differences in the parameters that characterize the shape, scale and tails of the frequency distributions. This suggests that significant uncertainties exist in the characterization of extreme precipitation, an issue that is highly important in the context of climate variability and change in South America.

Acknowledgements. L. M. V. Carvalho, C. Jones and B. Liebmann thank the support of NOAA's Climate Program Office (NA07OAR4310211 and NA10OAR4310170). L.M.V Carvalho, C. Jones, A. Posadas and R. Quiroz thank USAID-CIP (Sub-Contract SB100085). NCEP/NCAR Reanalysis and OLR data were provided by the NOAA/OAR/ESRL PSD, Boulder, Colorado, USA (www.esrl.noaa.gov). TRMM data was acquired by an international joint project sponsored by the Japan National Space Development Agency (NASDA) and the US National Aeronautics Space Administration NASA) Office of Earth Science. The help from Bob Dattore, NCAR-CISL, in providing the NCEP CFSR data is greatly appreciated.

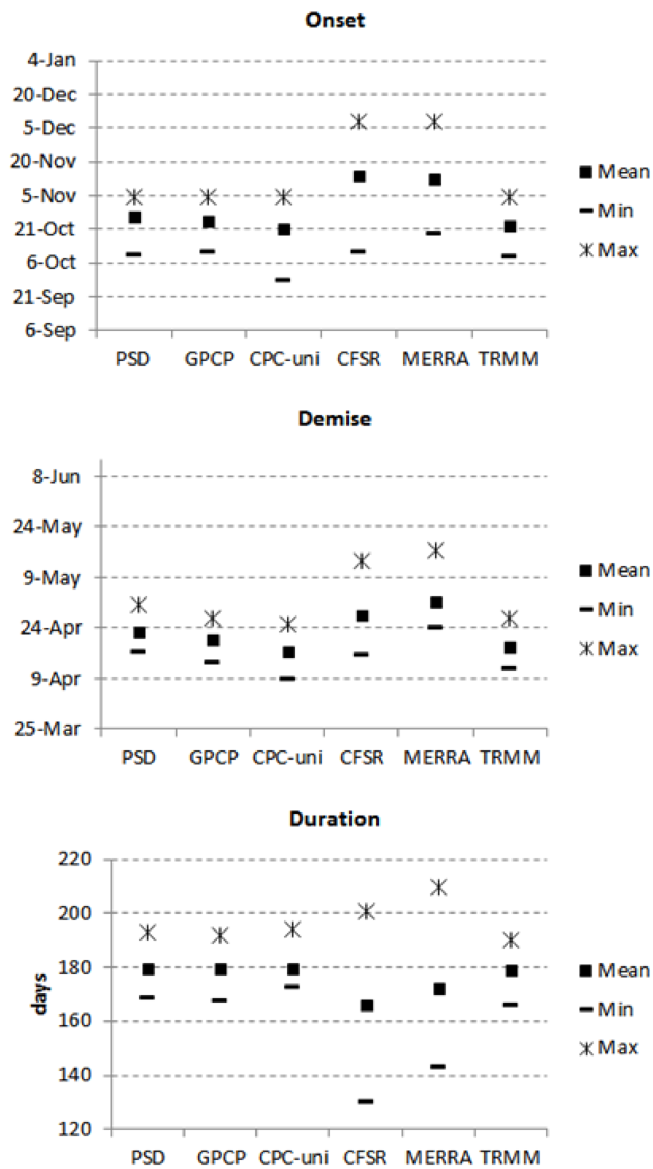

Fig. 2 Top: mean (squares), minimum (dash) and maximum (asterisk) dates of SAMS onset. Middle: mean (squares), minimum (dash) and maximum (asterisk) dates of SAMS demise. Bottom: mean (squares), minimum (dash) and maximum (asterisk) durations of SAMS. Data sets are indicated in the horizontal axis. Data sets have different grid spacings.

References

Bookhagen, B., and M. R. Strecker, 2008: Orographic barriers, high-resolution TRMM rainfall, and relief variations along the eastern Andes. *Geophys Res Lett*, **35,** -.

Bookhagen, B., and M. R. Strecker, 2010: Modern Andean rainfall variation during ENSO cycles and its impact on the Amazon Basin. Neogene history of Western Amazonia and its significance for modern diversity. C. Hoorn, H. Vonhof and F. Wesselingh. Oxford, U.K., Blackwell Publishing.

Bookhagen, B., and D. W. Burbank, 2011: Towards a complete Himalayan hydrologic budget: The spatiotemporal distribution of snow melt and rainfall and their impact on river discharge. *Journal of Geophysical Research-Earth Surface, doi:10.1029/2009JF001426, J Geophys Res-Earth, 115.*

Carvalho, L. M. V., C. Jones, A. N. Posadas, R. Quiroz, B. Bookhagen, and B. Liebmann, 2011: Precipitation characteristics of the South Monsoon System derived from multiple data sets. Journal of Climate (in review).

Chen, M. Y., W. Shi, P. P. Xie, V. B. S. Silva, V. E. Kousky, R. W. Higgins, and J. E. Janowiak, 2008: Assessing objective techniques for gauge-based analyses of global daily precipitation. *J. Geophys. Res.-Atmos.*, **113,** D04110, 04111-04113.

Dee, D. P., and Coauthors, 2011: The ERA-Interim reanalysis: configuration and performance of the data assimilation system. Quarterly Journal of the Royal Meteorological Society. *Quart. J. Roy. Meteor. Soc.*, **137,** 553–597, doi: 510.1002/qj.1828.

Gan, M. A., V. B. Rao, and M. C. L. Moscati, 2006: South American monsoon indices. *Atmos. Sci. Let.*, **6,** 219-223.

Grimm, A. M., C. S. Vera, and C. R. Mechoso, 2005: *The South American Monsoon System.* In: The American Monsoon Systems: An Introduction. C.-P. Chang, B. Wang and N.-C. G. Lau, Eds WMO/TD No. 1266 (TMRP Report No. 70), 197-206.

Higgins, R. W., W. Shi, E. Yarosh, and R. Joyce, 2000: Improved United States precipitation quality control system and analysis. *NCEP/Climate Prediction Center ATLAS No. 7,* National Oceanic and Atmospheric Administration, 40 pp.

Higgins, R. W., V. E. Kousky, V. B. S. Silva, E. Becker, and P. Xie, 2010: Intercomparison of Daily Precipitation Statistics over the United States in Observations and in NCEP Reanalysis Products. *J. Climate*, **23,** 4637-4650.

Horel, J. D., A. N. Hahmann, and J. E. Geisler, 1989: An investigation of the Annual Cycle of Convective Activity over the Tropical Americas. *J. Climate*, **2,** 1388-1403.

Huffman, G. J., and Coauthors, 2001: Global Precipitation at One-Degree Daily Resolution from Multisatellite Observations. *J. Hydrometeorol.*, **2,** 36-50.

Jones, C., and L. M. V. Carvalho, 2002: Active and break phases in the South American Monsoon System. *J. Climate*, **15**, 905-914.

Kousky, V. E., 1988: Pentad outgoing longwave radiation climatology for the South American sector. *Rev. Bras. Met.*, **3,** 217-231.

Legates, D. R., and C. J. Willmott, 1990: Mean Seasonal and Spatial Variability in Gauge-Corrected, Global Precipitation. *Int. J. Climatol.*, **10,** 111-127.

Liebmann, B., and D. Allured, 2005: Daily precipitation grids for South America. *Bull. Amer. Meteor. Soc.*, **86,** 1567-1570.

——, 2006: Daily precipitation grids for South America - Reply. *Bull. Amer. Meteor. Soc.*, **87,** 1096-1096.

Liebmann, B., and Coauthors, 2007: Onset and end of the rainy season in South America in observations and the ECHAM 4.5 atmospheric general circulation model. *J. Climate*, **20,** 2037-2050.

Marengo, J. A., B. Liebmann, V. E. Kousky, N. P. Filizola, and I. C. Wainer, 2001: Onset and End of the Rainy Season in the Brazilian Amazon Basin. *J. Climate*, **14,** 833-852.

Marengo, J. A., and Coauthors, 2010: Review: Recent developments on the South American monsoon system. *Int. J. Climatol.***,** DOI: 10.1002/joc.2254.

Rienecker, M. M., and Coauthors, 2011: MERRA - NASA's Modern-Era Retrospective Analysis for Research and Applications. *J. Climate***,** (in press).

Saha, S., and Coauthors, 2010: The NCEP Climate Forecast System Reanalysis. *Bull. Amer. Meteor. Soc.*, **91,** 1015-1057.

Silva, V. B. S., V. E. Kousky, and R. W. Higgins, 2011: Daily Precipitation Statistics for South America: An Intercomparison between NCEP Reanalyses and Observations. *J. Hydrometeorol.*, **12,** 101-117.

Silva, V. B. S., V. E. Kousky, W. Shi, and R. W. Higgins, 2007: An Improved Gridded Historical Daily Precipitation Analysis for Brazil. *J. Hydrometeorol.*, **8,** 847-861.

Vera, C., and Coauthors, 2006: Toward a unified view of the American Monsoon Systems. *J. Climate*, **19,** 4977-5000.

Zhou, J. Y., and K. M. Lau, 1998: Does a monsoon climate exist over South America? *J. Climate*, **11,** 1020-1040.